PRE-MAIN SEQUENCE STELLAR EVOLUTION WITH MASS LOSS

DILHAN EZER
Institute for Space Studies, Goddard Space Flight Center, NASA, New York, N.Y., U.S.A.

and

A. G. W. CAMERON
Belfer Graduate School of Science, Yeshiva University, New York, N.Y., U.S.A.

and

Institute for Space Studies, Goddard Space Flight Center, NASA, New York, N.Y., U.S.A.

(Received 27 April; in final form 26 June, 1970)

Abstract. A semi-empirical formulation is given of the rate of stellar mass loss by stellar winds. Evolutionary studies of stars in the pre-main sequence (T Tauri) stage are presented for a variety of rates of mass loss. It has been found that different mass loss rates produce only small changes in the positions of equal evolutionary time lines in HR diagrams. Thus it is concluded that the spread of points in HR diagrams of young clusters results from a spread in their times of formation. This is consistent with the initiation of star formation by violent hydrodynamic compression of a typical interstellar cloud.

1. Introduction

There has been a certain amount of discussion concerning the distribution of pre-main sequence stars in HR diagrams of young galactic clusters. Such clusters typically have a region containing more massive stars on the main sequence; the less massive stars tend to form a broad band on the cooler side of the main sequence, running parallel to it. It has been suspected that these stellar distributions could not be fitted by equal time lines in the theoretical evolutionary sequences of stars which do not lose mass (Herbig, 1962a, 1962b); this has been confirmed by Iben and Talbot (1966) and by Ezer and Cameron (1967). The alternatives have been either that not all of the stars were formed at the same time, or that the stars have suffered varying amounts of mass loss in the pre-main sequence evolution, which causes them to have a variety of different evolutionary tracks, but in principle may cause them to reach a position of lower luminosity and higher temperature in a faster time than is possible without mass loss. In this paper we examine the latter process.

The initiation of star formation is obviously a rather complex process. We discuss only some conceptual aspects of it, based upon the hypothesis that the gravitational collapse and fragmentation of individual interstellar clouds is the basic process. This has previously been discussed by one of us (Cameron, 1962).

We start with the principle of approximate pressure equilibrium in the interstellar medium (Spitzer, 1954; Field, 1969).

A typical H I cloud is likely to have a mass of $10^3\ M_\odot$ and a temperature of about

Astrophysics and Space Science **10** (1971) 52–70.

10^2 K and a density of ~ 10 atoms cm^{-3}. This defines the equilibrium pressure. If such a cloud were to become unstable against gravitational collapse at 10^2 K, it would need to be compressed to a density of $\sim 10^3$ atoms cm^{-3}, two orders of magnitude higher in pressure. Actually, the temperature would probably fall to about ~ 30 K, so that the threshold for collapse is reached at a few hundred atoms cm^{-3}. This pressure is still one order of magnitude higher than normal.

Large pressure excesses are produced in the interstellar medium when O or B stars are formed near HI clouds. The ionization of the surface layers of such a cloud will raise the temperature, and hence pressure, by two orders of magnitude, and the rocket-like recoil of the interior can thus lead the cloud to the threshold of gravitational collapse. Thus, the initiation of star formation is likely to be a violent hydrodynamic process.

At 10^2 K sound speed is about 10^5 cm/sec. A sound wave would traverse the radius of a 10^3 $M_\odot$ cloud of 10 atoms cm^{-3} and 10^2 K in about 5×10^6 yr. If the cloud were to start collapsing in free fall at the threshold for collapse, it would take 1.6×10^6 yr to complete the collapse (Cameron, 1962). Since the latter time is much shorter than the former, it would appear that the former time is a rough measure of the interval over which various parts of the cloud can go over into free-fall collapse. Rapid cooling of the cloud during collapse prevents one part from receiving pressure waves from another part, thus initiating fragmentation. Conservation of angular momentum causes the fragments to flatten into disks, but these dissipate into stars in times of the order of 10^3 yr (Cameron, 1969). Thus it is conceivable that the formation of stars in a cluster may spread out over $\sim 5 \times 10^6$ yr. We conclude from the analysis in this paper that such a spread in formation times apparently does occur.

The calculations reported in this paper are of stellar evolution in the pre-main sequence, or T Tauri phase. These calculations differ from those reported by us previously through incorporation of mass loss during the evolution. The mass loss rates are derived in a semi-empirical manner. The results are compared with the distribution of stars in HR diagrams of young galactic clusters.

2. Mass Loss from T Tauri Stars

T Tauri stars are believed to be very young newly-formed stars. There have been a number of review articles summarizing the observational properties of these stars (Herbig, 1962a, 1967; Kuhi, 1966a).

Large concentrations of these objects are found in the Orion Nebula, NGC 2264, NGC 7000 and other extremely young clusters.

T Tauri stars are losing mass. The emission lines of many of these stars have violet-displaced absorption features which have been interpreted as due to material moving away from stellar surfaces and leaving the stars, since no sign of its return is present in the spectra.

Kuhi (1964, 1966b) has computed the rate of mass loss from eight T Tauri stars by analyzing the broad emission line profiles of H and CaII in their spectra. He assumed

that the expanding envelope is spherically symmetrical with the ejected atoms all having the same initial velocity and being subject only to gravitational forces.

The emitting region is surrounded by a thin outward moving shell which produces violet-displaced absorption components. With suitable estimates of the radius and effective temperature and a fit of the computed profiles to the observed contours, it is possible to estimate the rate of mass loss from these stars. In Table I we summarize some characteristics and computed mass loss rates from the T Tauri stars which Kuhi studied.

TABLE I

Properties of T Tauri stars

Star	$M/M_\odot$	$R/R_\odot$	Mass Loss ($10^7\ M_\odot\ \mathrm{yr}^{-1}$)	Mass Loss Parameter α
RY Tau	0.90	3.25	0.31	1.53×10^{-9}
T Tau	0.60	4.56	0.35	2.21×10^{-10}
GW Ori	1.30	8.64	0.35	7.06×10^{-11}
RU Lup	1.42	2.95	1.42	7.85×10^{-9}
AS 209	0.81	2.94	0.65	2.11×10^{-9}
LK Hα 120	4.10	11.64	5.85	1.73×10^{-9}
SU Aur	1.21	5.68	0.25	1.65×10^{-10}
RW Aur	1.16	2.46	1.11	8.57×10^{-9}

3. Chemical Composition

One of the motivations for this work was to determine how much mass the Sun might have lost during its gravitational contraction phase. Therefore a proper composition for solar material has to be chosen. The present estimate of the composition has been obtained in the following way.

Studies of solar cosmic rays have been given the ratio of helium to oxygen in the Sun as 107 ± 14 (Biswas *et al.*, 1963). It has been generally believed that the cosmic ray ratio of helium to oxygen should reflect the true helium/oxygen ratio in solar material. Actually, revised spectroscopic determinations of the ratios of carbon, nitrogen and oxygen in the Sun are in good agreement with solar cosmic ray determinations (Lambert, 1967). It appears that the abundances of elements in Type I carbonaceous chondrites represent the characteristics of the non-volatile constituents of primitive solar matter rather well (Cameron, 1968). Therefore, taking revised spectroscopic values for carbon, nitrogen and oxygen (Lambert, 1968) and the solar cosmic ray ratio of helium/oxygen and neon/oxygen, and meteoritic abundances of the other light elements (Cameron, 1968), we obtained a solar composition, in terms of the mass fractions of hydrogen, helium and heavy elements, as $X=0.787$, $Y=0.197$ and $Z=0.016$.

A test of a satisfactory helium/hydrogen ratio in the Sun is to show that, with the composition determined in this way, solar evolution should produce the present-day luminosity at the end of 4.5×10^9 yr, the accepted age of the solar system.

Using the above composition for the initial solar matter, the evolution of the Sun was followed from the point where the collapsing proto-sun became stable against dynamical collapse, up to its present age, 4.5×10^9 yr. At the end of 4.5×10^9 yr a lower luminosity was obtained for the present Sun. A higher luminosity can be achieved by assuming a higher value for the helium content.

With different trial values of the initial He abundance in the solar material, and of l/H, the ratio of the mixing-length to pressure scale height, for the treatment of turbulent motions of the convecting elements in the structure of the Sun, the present characteristics of the Sun were well represented by an initial composition,

$$X = 0.762, \quad Y = 0.223, \quad \text{and} \quad Z = 0.015, \quad \text{and for} \quad l/\mathrm{H} = 1.3 .$$

The abundances of selected elements for this solar composition are given in Table II. Selected model characteristics from the calculated evolutionary sequence of solar models without mass loss are summarized in Table III. The first column gives the evolution time in years, taking the threshold of stability as zero; the second, third, fourth and fifth columns give radius, luminosity in solar units, central temperature T_c and density ϱ_c. The last column gives the hydrogen abundance X_1, by mass, at the center of the Sun.

It is worth while to note that, in the present evolutionary study, the Sun starts to develop a radiative core after about 1.5 million years. The outer convection zone in

TABLE II

Abundances of selected elements

Element	Mass Fraction	Relative Numbers	Source
H	0.762	3.44×10^{10}	Sun, relative to Si
He	0.223	2.53×10^{9}	Solar evolution
C	3.24×10^{-3}	1.22×10^{7}	Sun
N	9.13×10^{-4}	2.95×10^{6}	Sun
O	7.22×10^{-3}	2.04×10^{7}	Sun
Ne	9.10×10^{-4}	2.04×10^{6}	Solar cosmic rays
Na	3.22×10^{-5}	6.32×10^{4}	Chrondrites
Mg	5.64×10^{-4}	1.05×10^{6}	Chrondrites
Al	5.06×10^{-5}	8.51×10^{4}	Chrondrites
Li	6.21×10^{-4}	1.00×10^{6}	Chrondrites
P	8.76×10^{-6}	1.27×10^{4}	Chrondrites
S	3.59×10^{-4}	5.06×10^{5}	Chrondrites
Cl	1.95×10^{-6}	1.97×10^{3}	Chrondrites
Ar	2.02×10^{-4}	2.28×10^{5}	Interpolated
K	2.92×10^{-6}	3.24×10^{3}	Chrondrites
Ca	6.52×10^{-5}	7.36×10^{4}	Chrondrites
Ti	1.95×10^{-6}	2.30×10^{3}	Chrondrites
Cr	1.46×10^{-5}	1.24×10^{4}	Chrondrites
Mn	1.07×10^{-5}	8.80×10^{3}	Chrondrites
Fe	1.10×10^{-3}	8.90×10^{5}	Chrondrites
Co	2.92×10^{-6}	2.30×10^{3}	Chrondrites
Ni	5.95×10^{-5}	4.57×10^{4}	Chrondrites

TABLE III

Evolutionary sequence of solar models

(Initial composition $X_1 = 0.762$, $Z = 0.015$, $l/H = 1.3$, $R_\odot = 6.91 \times 10^{10}$ cm, $L_\odot = 3.90 \times 10^{33}$ erg sec^{-1})

Time	$R/R_\odot$	$L/L_\odot$	T_cK	ϱ_cg cm^{-3}	X_1
1.20×10	5.95×10^{1}	4.50×10^{2}	1.44×10^{5}	7.31×10^{-5}	0.762
1.80×10^{2}	4.88	3.31	1.73	1.23×10^{-4}	0.762
1.14×10^{3}	3.28	1.78	2.50	3.56	0.762
1.42×10^{4}	1.44	4.78×10^{1}	5.40	3.50×10^{-3}	0.762
1.19×10^{5}	6.53×10^{0}	1.24	1.15×10^{6}	3.38×10^{-2}	0.762
5.61	3.65	4.33×10^{0}	2.04	1.86×10^{-1}	0.762
1.35×10^{6}	2.69	2.41	2.76	4.57	0.762
4.49	1.78	1.02	4.01	1.67×10^{0}	0.762
9.21	1.42	0.65	4.87	4.17	0.762
1.55×10^{7}	1.26	0.55	5.66	8.27	0.762
4.07	1.09	0.75	9.13	4.54×10^{1}	0.762
4.70	1.07	0.92	1.07×10^{7}	6.95	0.762
6.58	0.90	0.73	1.32	7.98	0.761
7.84	0.89	0.71	1.32	8.19	0.760
1.10×10^{8}	0.89	0.72	1.33	8.45	0.758
2.48	0.89	0.74	1.33	8.73	0.749
5.50	0.90	0.75	1.34	8.99	0.729
7.52	0.90	0.76	1.34	9.12	0.717
1.15×10^{9}	0.91	0.78	1.36	9.49	0.690
2.16	0.94	0.84	1.40	1.06×10^{2}	0.619
3.17	0.96	0.90	1.44	1.21	0.541
3.57	0.97	0.93	1.47	1.28	0.509
4.17	0.99	0.98	1.50	1.39	0.458
4.50	1.00	1.00	1.52	1.47	0.429

TABLE IV

Neutrino fluxes at one AU (cm^{-2} sec^{-1}) from the indicated sources

$^1H + {}^1H$	^7Be	^8B	^{13}N	^{15}O
6.64×10^{10}	3.14×10^{9}	0.39×10^{7}	3.11×10^{8}	2.39×10^{8}

the present Sun covers only a mass fraction of $3.5 \times 10^{-3}\ M_\odot$. A small convective core develops at an evolution time of 5×10^{7} yr due to the sudden onset of nuclear burning and extends over 9% of the mass. It diminishes in size during further evolution and entirely disappears at the end of 2×10^{9} yr. Thus, the model for the present Sun has no convection core. In Table IV, the neutrino fluxes at one astronomical unit from the Sun, which have been calculated by using the last model representing the present Sun, are also given.

As a result of this evolutionary study of the Sun the initial solar material requires a ratio of helium to oxygen of 120.5, which is within the uncertainty of the solar cosmic ray determination. The neutrino flux from ^8B is 3.9×10^{6} cm^{-2} sec^{-1}. At present, the experimental results of R. Davis give only an upper limit to the flux of ^8B neutrinos

of 2×10^6 cm^{-2} sec^{-1}. Our theoretical results exceed his value by a factor of 2. The source of this discrepancy is not known, but it is of the same order as that currently obtained by other investigators (Iben, 1969).

4. Opacity

The opacity of the material was obtained by interpolation between three sets of opacity tables for mixtures in which hydrogen to helium ratios change, but heavy elements stay constant. The tables are stored in the computer for a range of densities of temperatures of interest. These opacities were obtained from the Cox opacity code, made available to the Institute for Space Studies. The Institute version of the Cox opacity program does not include the effects of bound-bound (line) absorption. Appropriate corrections to the continuous opacity, due to lines, have been applied by comparing the contribution of the line opacity to the continuous opacity in the opacity calculations previously provided to us by J. Stewart for different mixtures.

Recently, it has been shown that the lines due to auto-ionizing states also substantially contribute to the total opacity at temperatures greater than about 5×10^5 K (Watson, 1969). Watson gives continuous opacity, continuous plus normal line opacity, and continuous plus auto-ionization plus normal line opacity separately, for the mixture $X = 0.739$, $Z = 0.021$.

Appropriate corrections to our opacity tables have been made using ratios of opacities from the work of Watson.

5. Energy Generation

The sources of energy generation used in these computations are the same as in our previous work on the evolution of the Sun (Ezer and Cameron, 1965). However, the nuclear parameters used are different. The cross-section constant for the proton-proton reaction was taken to be $S_{11} = 3.78 \times 10^{-22}$ keV-b (Bahcall and May, 1968), and for the reaction $^7\mathrm{Be}(p, \gamma)^8\mathrm{B}$, $S_{71} = 3.5 \times 10^{-2}$ keV-b (Parker, 1968). The other reaction rates are taken from the recent review by Fowler *et al.* (1967). The ^{7}Be capture rate was taken from recent work by Bahcall and Moller (1969).

6. Rate of Mass Loss

There is a great deal of observational evidence concerning mass loss in stars, both before and after the main sequence (Deutsch, 1960a, b, 1969; Weymann, 1963). However, there are very few quantitative measurements of mass loss rates, and this hampers the following consideration more than we would like.

There appear to be two principal types of stellar mass loss. High temperature supergiant stars can lose mass at a large rate, and this is probably due to the effects of radiation pressure. We do not consider this mechanism in what follows, because our calculations do not include stars of this kind. The second mechanism is stellar wind.

We assume that the large mass loss rates in red giant stars and in T Tauri stars are due to the stellar wind mechanism, although this has not been demonstrated with a high degree of certainty.

Stellar winds arise from a mechanical heating of the stellar corona. Acoustic, gravity and hydromagnetic waves can, in principle, be responsible for this heating. However, the relative role that these waves play in heating the solar corona is still largely conjectural. In any case, it is not at present possible to construct a reliable model of the solar corona taking these heating effects properly into account. The mass loss rate is a sensitive function of the coronal temperature, so that even if such a model could be constructed, it is unlikely that the mass loss rate could be reliably predicted. Indeed, since a high rate of mass loss would modify the coronal structure, it seems likely that the stellar wind is partly self-regulated for any assumed stellar condition.

Therefore, in order to carry out stellar evolution calculations with mass loss taken into account, we have been forced to formulate the mass loss rate in a semi-empirical manner. Let us try to extract some of the relevant physical parameters from the problem, and to leave the unknown parameters as a function to be evaluated from observations. Since the mechanical wave generation originates at the surface of the convective zone just below the photosphere, the mass loss is probably proportional to the surface area of the star, or to R^2. Neglecting the kinetic energy at infinity of the ejected mass, the mass loss rate will be inversely proportional to the potential energy per gram at the stellar surface, GM/R. Hence, we write the mass loss as

$$\frac{dM}{dt} = -\alpha \frac{R^3}{M}, \tag{1}$$

where α is the unknown function to be evaluated from observations. We shall customarily take R and M to be in present solar units and express α in units of solar masses per year.

For the present average solar wind (Parker, 1963a, b) the mass loss rate is about $\alpha = 3 \times 10^{-14}\ M_\odot\ \mathrm{yr}^{-1}$.

For the red giant star α Herculis, Weymann (1926) has reinterpreted the observations of Deutsch (1956). This star has a radius of 580 $R_\odot$, but the mass is uncertain and might lie in the range 15 to $2M_\odot$, with somewhat higher values probably being preferred. Hence $4.65 \times 10^{-14} > \alpha > 6.15 \times 10^{-15}\ M_\odot\ \mathrm{yr}^{-1}$. Similarly, from Weymann's discussion of α Orionis, we infer $\alpha = 7.76 \times 10^{-14}\ M_\odot\ \mathrm{yr}^{-1}$.

Thus for the middle main sequence and for post-main sequence giants, we may take roughly $\alpha \sim 3 \times 10^{-14}\ M_\odot\ \mathrm{yr}^{-1}$. This number is to be regarded as very uncertain.

For the red dwarf YZ Canis Minoris, Lovell (1969) finds a radius of 0.25 $R_\odot$ and a mass of 0.3 $M_\odot$, and from the discussion of Kahn (1969) on the mass loss, we find $\alpha = 5.75 \times 10^{-11}\ M_\odot\ \mathrm{yr}^{-1}$.

In Table I we have listed the values of α for the T Tauri stars whose characteristics are given there. It may be seen that $10^{-8} > \alpha > 10^{-10}\ M_\odot\ \mathrm{yr}^{-1}$. We believe that much of this range of variation of α is real.

It is clear that the T Tauri stars are losing mass at a much greater intrinsic rate than they will later on the main sequence and after it. This suggests that they possess considerably larger magnetic fields than they will have at a later time, so that hydromagnetic heating effects are greatly enhanced in the corona. These magnetic fields must decrease with time. The decrease is obviously rapid in the case of the massive red giant stars α Herculis and α Orionis, which are unlikely to possess outer convection zones on the main sequence. There has evidently been time for the excess field to decay in the Sun, which has an outer convection zone containing about 0.0035 $M_\odot$. We do not know the age of YZ Canis Minoris, but we note that it must be fully convective, and it appears that the excess magnetic field has only partly decayed.

We have attempted to take these features into account by writing our final mass loss formula in the form

$$\frac{dM}{dt} = -(3 \times 10^{-14} + \alpha \exp - t/\tau)\frac{(R/R_\odot)^3}{(M/M_\odot)}. \tag{2}$$

We have made a rough estimate of the decay constant τ taking into account the observation of Wilson (1959, 1963) on the rate of decrease of chromospheric activity with increasing stellar age, which seems to be another manifestation of these phenomena. The result is

$$\tau = 5.7 \times 10^9 \, f_m \, \mathrm{yr}, \tag{3}$$

where f_m is the mass fraction in the outer convection zone. Equations (2) and (3) roughly reproduce the observational information on stellar mass loss rates discussed above.

7. Computations

The computations described here were carried out with a new stellar evolution program, rewritten using logarithmic physical variables in the stellar structure equations. The numerical integrations of the differential equations of stellar structure were carried out by the Henyey method. The main modification of the program from our previous work, besides using logarithmic variables, was to apply the Henyey method from the center all the way to the surface. This procedure does not require a separate program for the atmospheric calculations. The same equations can be used throughout the star or in any desired region of the star. The procedure has the advantage that the time-dependent energy flow equation which defines the luminosity of the star

$$\frac{dL_r}{dM_r} = \varepsilon_{\mathrm{Nuc}} - \frac{\partial E}{\partial t} - P\frac{\partial}{\partial t}\left(\frac{1}{\varrho}\right)$$

can be handled properly in the outermost part of the star where most of the mass is lost. For ease of calculation, the loss of mass between successive evolutionary models is spread over several of the outermost zones. Therefore, the equations not only

involve time-derivatives, but also mass-derivatives, e.g.,

$$\frac{dE}{dt} = \frac{\partial E}{\partial t} + \frac{\partial E}{\partial m}\left(\frac{dm}{dt}\right). \tag{4}$$

In the far interior, the time-dependent changes of physical variables arise from the nuclear evolution of the star. Since the mass loss occurs in the region of the star where the nuclear energies are unimportant, no change is required for the equations governing the change of composition of the star.

When a model at a time step n is obtained, the amount of mass to be lost during the coming time step, $n+1$, is calculated from the Equation (2). Because of computational difficulties, the fractional mass loss per time step should be limited. We have found that for $|\Delta M/M| \sim 0.02$, the convergence of the model is not much affected by the mass loss.

We assume that, during a time step, the energy required to eject the mass is

$$L_{\text{mass}} = \frac{GM}{R}\left|\frac{dM}{dt}\right| \text{ erg/sec}.$$

Then the energy output per second in the form of radiation is

$$L = L_{\text{Total}} - L_{\text{mass}}.$$

This will cause a decrease of surface luminosity and, through the relation $L = 4\pi R^2 \sigma T_e^4$, a drop in the effective temperature. This correction is especially important when the mass loss rate is large in the early models computed.

We did not consider any correction to the pressure due to the mass ejection. Actually, when the mass ejection mechanism is operative, it becomes questionable whether the hydrostatic equation should be used. Therefore, for this exploratory study, the neglect of any correction to the pressure is quite justified.

The removal of mass from the zones has been carried out in the following way.

Suppose that the total mass of the star at the time step M is M_T.

Define $\eta_i \equiv M_i/M_T$ where M_i = mass at the point i. $f(\eta_i)$ gives the fraction of the mass loss occurring at the point corresponding to η_i. Let η_1 and η_2 be such that $f(\eta) = 0$ for $\eta \leqslant \eta_1$ and $\eta \geqslant \eta_2$; then $f(\eta)$ is subject to the condition that

$$\left.\begin{aligned} &f(\eta_1) = 0, \\ &f(\eta_2) = 0, \\ &\int_{\eta_1}^{\eta_2} f(\eta)\, d\eta = \Delta M, \end{aligned}\right\} \tag{A}$$

where ΔM is the total amount of mass lost.

The total mass loss occurring below point i is

$$\int_{\eta_1}^{\eta_i} f(\eta)\, d\eta .$$

Therefore,

$$\Delta M_i^{n+1} = \Delta M_i^n - \int_{\eta_i - 1}^{\eta_i} f(\eta)\, d\eta .$$

For the $f(\eta)$ function a quadratic equation such as

$$f(\eta) = a\eta^2 + b\eta + c$$

has been chosen and the coefficients are defined with the condition (A).

Our experience shows that it is desirable to start the mass removal procedure not at the surface, where the mass fraction in each zone is very small, but somewhere near $M_i = 0.995\ M_T$. Therefore, η_1 is taken as 0.995. As far as η_2 is concerned, it is left as a parameter. For the wholly convective models which correspond to the early evolutionary phases of the stars, η_2 was taken as 0.90. Thus the mass was taken out from only the outer 10% of the star's mass. With further evolution, when the star starts to develop radiative zones near the center, and the bottom of the convective zone recedes toward the surface of the star, so that the center radiative zone covers more than 90% of the star's mass, η_2 is taken as the mass fraction at the bottom of the convective zone. In this way the mass removal produce has been confined inside the outer convective zone of the star.

8. Computational Results

The evolutionary study of stars with mass loss was carried out with the solar composition in which $X = 0.762$, $Z = 0.015$, as described earlier in this paper. The ratio of mixing length to pressure scale height was 1.3.

The first series of calculations was performed by assuming that solar material contains no initial amount of deuterium. In these calculations the evolutionary study was started at the point called the 'threshold of stability' from energy considerations (Ezer and Cameron, 1967). Taking the initial mass at this point as 5 $M_\odot$, 3 $M_\odot$, 1.6 $M_\odot$ and 1$M_\odot$, and the coefficient α in Equation (2), which defines the mass loss rate, equal to 10^{-10}, the evolution of the stars was followed through the gravitational contraction phase, approach to the main sequence, and hydrogen burning phases. $\alpha = 10^{-10}$ gives a very small amount of mass loss during the evolution. The stars of 5 $M_\odot$, 3 $M_\odot$, 1.6 $M_\odot$ and 1 $M_\odot$ reach the zero-age main sequence as stars of 4.75 $M_\odot$, 2.81 $M_\odot$, 1.48 $M_\odot$ and 0.90 $M_\odot$, respectively. Taking the time as zero at the threshold of stability, the zero-age main sequence time for the stars is, in turn, 2×10^6 yr, 9×10^6 yr, 4×10^7 yr, and 1.3×10^8 yr.

A second series of calculations was carried out taking the masses as 5 $M_\odot$, 3 $M_\odot$ and 1.6 $M_\odot$, and the coefficient α in the mass loss formula as 10^{-9}. The results of these evolutionary studies have been plotted in Figure 1. The evolutionary tracks with constant mass were also plotted for comparison. The evolutionary tracks with constant mass were calculated for the mixture in which $X=0.739$, $Z=0.021$, and the ratio of

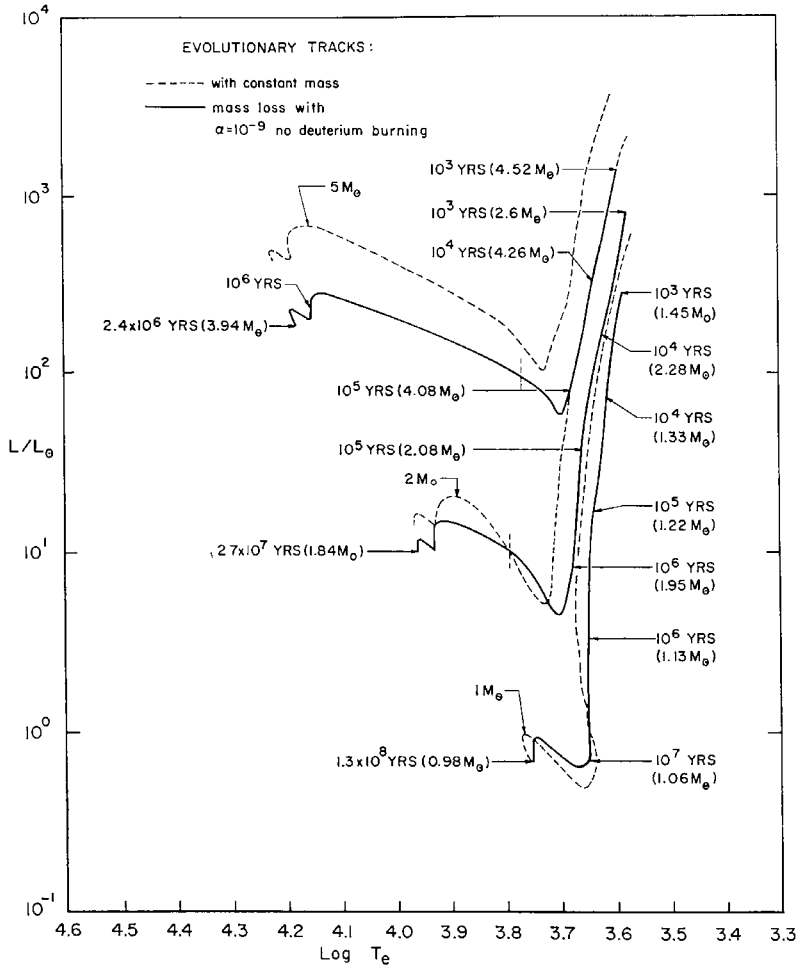

Fig. 1. The theoretical Hertzsprung-Russell diagram for stars of different masses losing mass at a rate $\alpha = 10^{-9}$ with no deuterium in the initial material. The horizontal arrows indicating the last points of the tracks give the zero-age main sequence times; final masses are also given in parentheses. The evolutionary tracks with dashed lines are those obtained from the evolution of constant mass stars of 1 $M_\odot$, 2 $M_\odot$ and 5 $M_\odot$.

mixing length to pressure scale height is 2. The new composition and mixing length ratio used in the present study would have resulted in a decrease in the effective temperatures of the fully convective tracks. In the figure, the reduced masses of the stars during their evolution, and the corresponding evolution times, have been indicated. The short vertical dashed lines crossing the evolutionary tracks show the places where the stars become fully radiative. From there on, there is no stellar mass loss and the evolution takes place at constant mass. The star with initial mass 5 $M_\odot$ becomes fully

radiative in about 6×10^5 yr, with a mass of 3.94 $M_\odot$. The star of 3 $M_\odot$ stops having an outer convection zone in about 9×10^6 yr, and reaches the main sequence as a star of 1.84 $M_\odot$. The star with the initial mass 1.6 $M_\odot$ maintains an outer convection zone when it reaches the zero-age main sequence as a star of 0.98 $M_\odot$; therefore, it keeps losing mass throughout its evolution.

Another series of calculations was performed assuming that the stellar material contains the terrestrial ratio of deuterium to hydrogen. For this series of calculations, the evolutionary tracks have been constructed using a larger range of values of α. For computational convenience, it was assumed that the stars start to lose mass after an evolution of about 10^4 yr. From there on, the mass ejection rate obeys the relation given by Equation (2). The results are summarized in Figures 2 and 3. In these figures

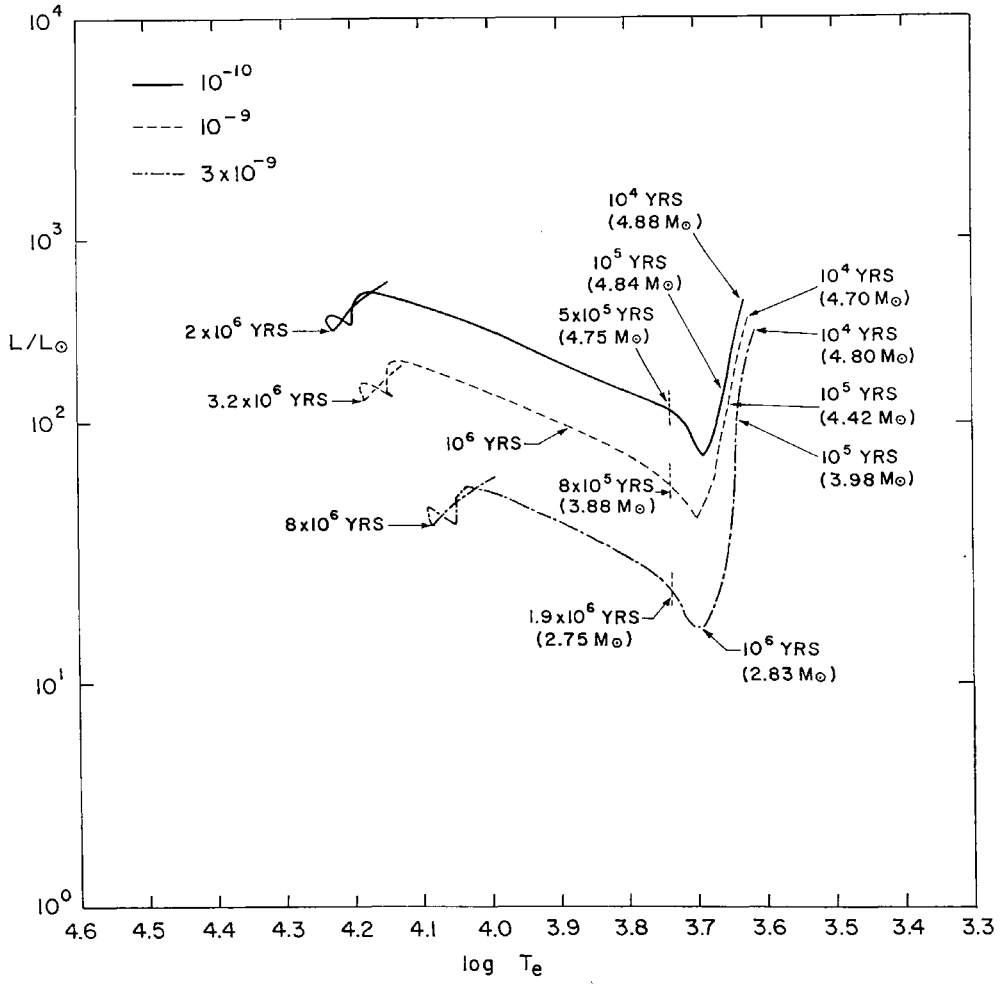

Fig. 2. The theoretical Hertzsprung-Russell diagram for the deuterium burning models with initial masses of 4.88 $M_\odot$, 4.80 $M_\odot$ and 4.70 $M_\odot$ and with different rates of mass loss, in the gravitational contraction stage, in the approach to the main sequence, and on the main sequence. The dashed vertical lines crossing the evolutionary tracks indicate the points where the stars stop having outer convection zones; the masses at that point are also given in parentheses. From there on the evolutionary tracks are those obtained for the stars with constant masses of 2.75 $M_\odot$, 3.88 $M_\odot$ and 4.75 $M_\odot$. The horizontal arrows on the left-hand side of the figure give zero-age main sequence times.

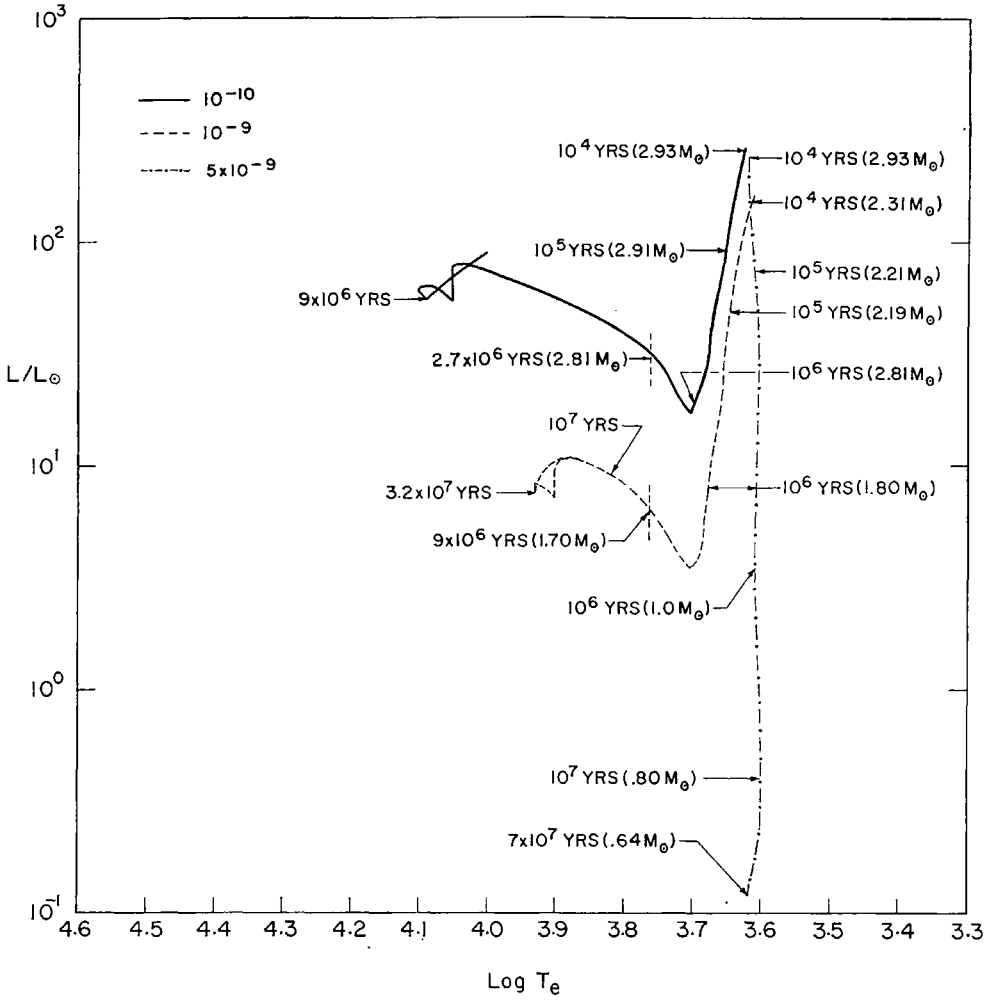

Fig. 3. The theoretical Hertzsprung-Russell diagram for the deuterium burning models with initial masses of 2.93 $M_\odot$ and 2.31 $M_\odot$ and with the mass loss rate indicated in the figure. The explanation of the figure is the same as for Figure 2.

the initial mass at 10^4 yr and the reduced mass at certain evolution times are indicated on the evolutionary tracks for the different values of α. The horizontal arrows on the left-hand side of the figure are the zero-age main sequence times for each track. The general nature of the evolution is very similar to that found for evolution at constant mass (Ezer and Cameron, 1967). It is interesting to note that for $\alpha = 5 \times 10^{-9}$, the star with initial mass 2.93 $M_\odot$, loses about 2.29 $M_\odot$ in about 7×10^7 yr and keeps losing mass due to the existence of the outer convection region.

In Table V, some results of interest for the evolution of the Sun with mass loss are tabulated. In this table, the evolution times and corresponding masses are given for different mass loss rates of the initial solar material contains either no deuterium or deuterium. From an inspection of the table, it can be seen how much mass the Sun might have lost during its gravitational contraction phase.

TABLE V

No Deuterium				With Deuterium			
$\alpha = 10^{-10}$		$\alpha = 10^{-9}$		$\alpha = 10^{-10}$		$\alpha = 10^{-9}$	
Time (yr)	$M/M_\odot$	Time (yr)	$M/M_\odot$	Time (yr)	$M/M_\odot$	Time (yr)	$M/M_\odot$
1.4×10^4	1.59	1.1×10^4	1.32	1.6×10^4	1.56	1.2×10^4	1.35
1.1×10^5	1.55	1.0×10^5	1.22	1.3×10^5	1.55	1.2×10^5	1.27
1.2×10^6	1.54	1.1×10^6	1.13	1.0×10^6	1.49	1.0×10^6	9.68×10^{-1}
1.2×10^7	1.53	1.6×10^7	1.05	1.0×10^7	1.48	1.3×10^7	8.79×10^{-1}
1.2×10^8	1.52	1.0×10^8	9.85×10^{-1}	1.0×10^8	1.48	1.0×10^8	8.09×10^{-1}
		1.1×10^9	9.80×10^{-1}			1.2×10^9	7.15×10^{-1}
		4.9×10^9	9.79×10^{-1}			4.5×10^9	7.03×10^{-1}

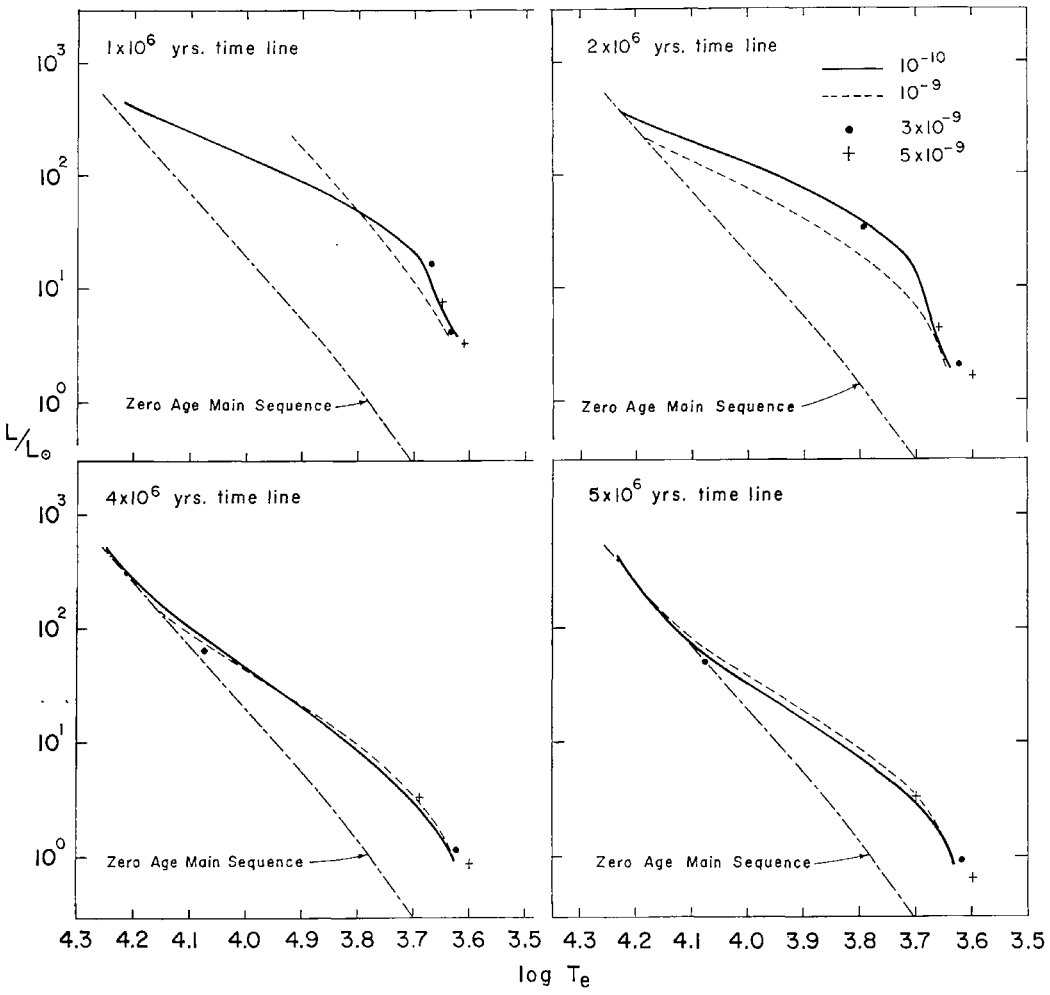

Fig. 4. The theoretical equal age lines for deuterium burning models with different rates of mass loss. The dots indicate the positions of the stars at the same age evolving with the mass loss rate of 3×10^{-9}, while the crosses correspond to a rate of 5×10^{-9}.

9. Comparison with Young Clusters

The results of evolutionary study of stars with mass loss allow us to draw theoretical lines of equal evolutionary time in the Hertzsprung-Russell diagram. In Figure 4 the time lines corresponding to 10^6, 2×10^6, 4×10^6 and 5×10^6 yr are shown by dotted lines for the evolutionary study with a mass loss rate of 10^{-9}, and by solid lines for a mass loss rate of 10^{-10}. The dots indicate the positions of the stars at the same age if they were evolved with a mass loss rate of 3×10^{-9}, while the crosses refer to a rate of 5×10^{-9}. From an inspection of the figure it can be seen that the largest separation of the constant time lines for different parameters α, occurs for near 2 – 3 million years.

In order to compare observational data with theory, the young cluster NGC 2264 and the extremely young cluster, Orion, have been chosen.

Figure 5 shows the positions of the stars in NGC 2264 in the theoretical Hertzsprung-Russell diagram. This cluster was extensively studied by Walker (1956, 1957). The bars indicate the stars with Hα emission. NGC 2264 has been compared with theoretical evolutionary studies with constant mass by many investigators. (See for example: Penston, 1964; Iben and Talbot, 1966; Ezer and Cameron, 1967). Superimposed on Figure 5 are 6×10^6 yr time lines with different parameters α obtained from theoretical model calculation of contracting stars with mass loss. The theoretical zero-age main sequence is indicated by dashes and dots. Although, from the turn-off point, an age of roughly 6×10^6 yr can be assigned for this cluster, the observed distribution of the stars still cannot be explained with the mass loss effect. The Orion Association has been studied by a number of investigators (Parenago, 1954; Sharpless, 1952, 1954, 1962; Johnson, 1957; and Morgan and Lodén, 1966). Walker (1969) recently presented three-color photoelectric observations of the stars in the vicinity of the Orion Nebula. This Nebula is one of the most favorable for comparison of the results of theoretical studies with observations. As Walker pointed out, besides being the nearest one, as in the case of NGC 2264, the entire cluster is seen projected against a dark cloud. Figure 6 shows the theoretical HR diagram for the clusters of stars associated with the Orion Nebula. For transformation of Walker's 1969 observational data to the theoretical HR diagram, the distance modulus of the cluster is taken as 8.37 magnitudes. The relations between (B−V) color index, bolometric correction and effective temperature are taken from Table II of Johnson (1966). In this figure, dots represent stars plotted according to their observed magnitude and colors, circles, stars corrected for differential reddening. Double stars given in Table II of Walker (1969) are first corrected for the effect of their companions, then plotted in the diagram by filled triangles if they have uniform reddening, and by open triangles if they are corrected for differential reddening. Vertical lines through the symbols indicate known variables, while horizontal lines represent stars with Hα emission. Zero-age main sequence and 3×10^6 yr time lines from the theoretical studies of contracting stars with different mass loss rates are also indicated on the figure. The theoretical study was performed with the solar conposition in which the heavy element abundance

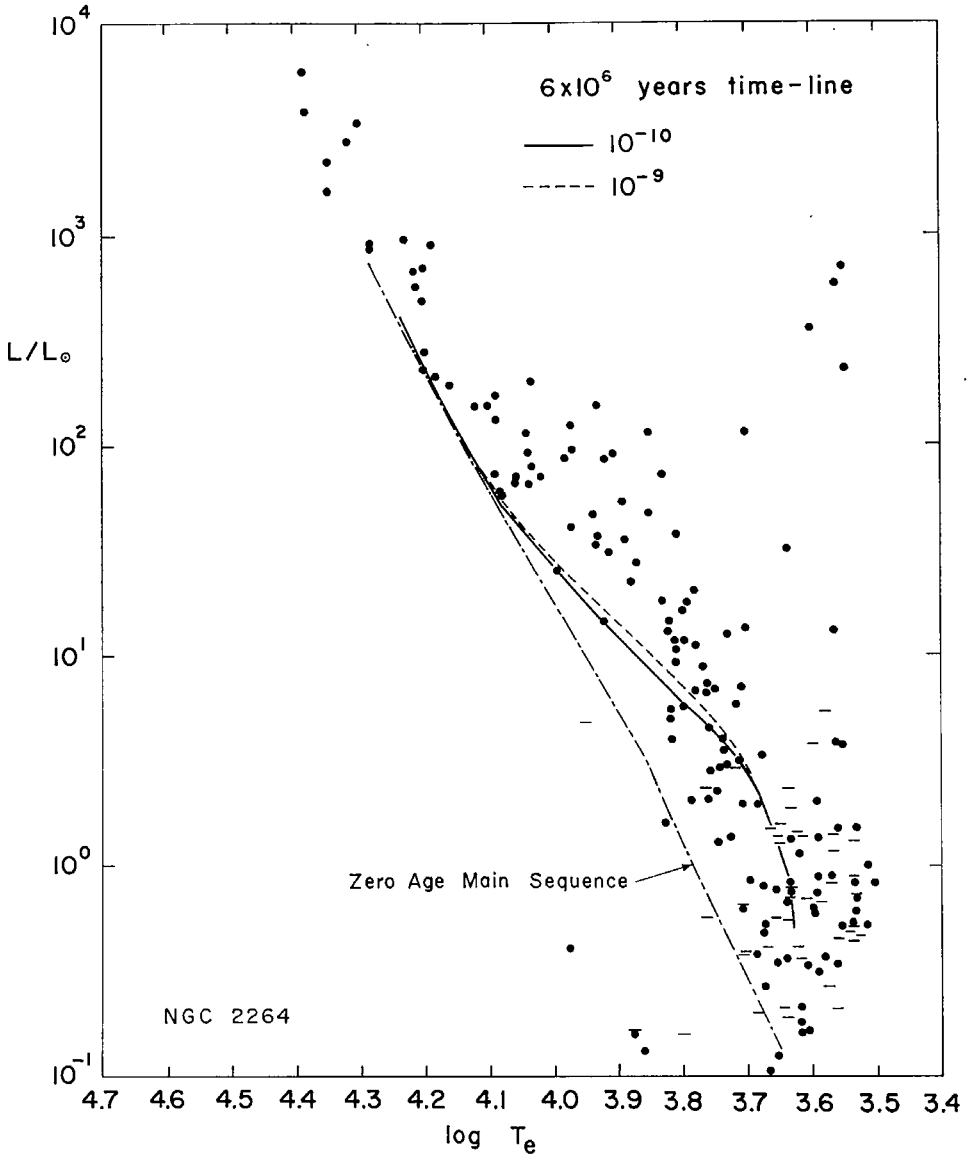

Fig. 5. The theoretical 6×10^6 yr time lines obtained by the evolutionary study of the stars with different rates of mass loss and the observed Hertzsprung-Russell diagram for the young cluster NGC 2264.

is 0.015. Since the Orion Nebula is an extremely young association of stars, the interstellar medium may have been enriched by the time of their formation. An increase in the heavy element content requires reddening of the main sequence position. 3×10^6 yr is the largest age which can be assigned to the Orion Nebula from the turn-off point. Even though the separation of the 3×10^6 yr time lines for different values of α is largest, the spread in the positions of the points in the diagram is much too large to be attributed to different rates of mass loss.

It is interesting to note the stars near the righthand edge of the diagram. These stars appear to be near the base of or on the Hayashi portion of their evolutionary tracks.

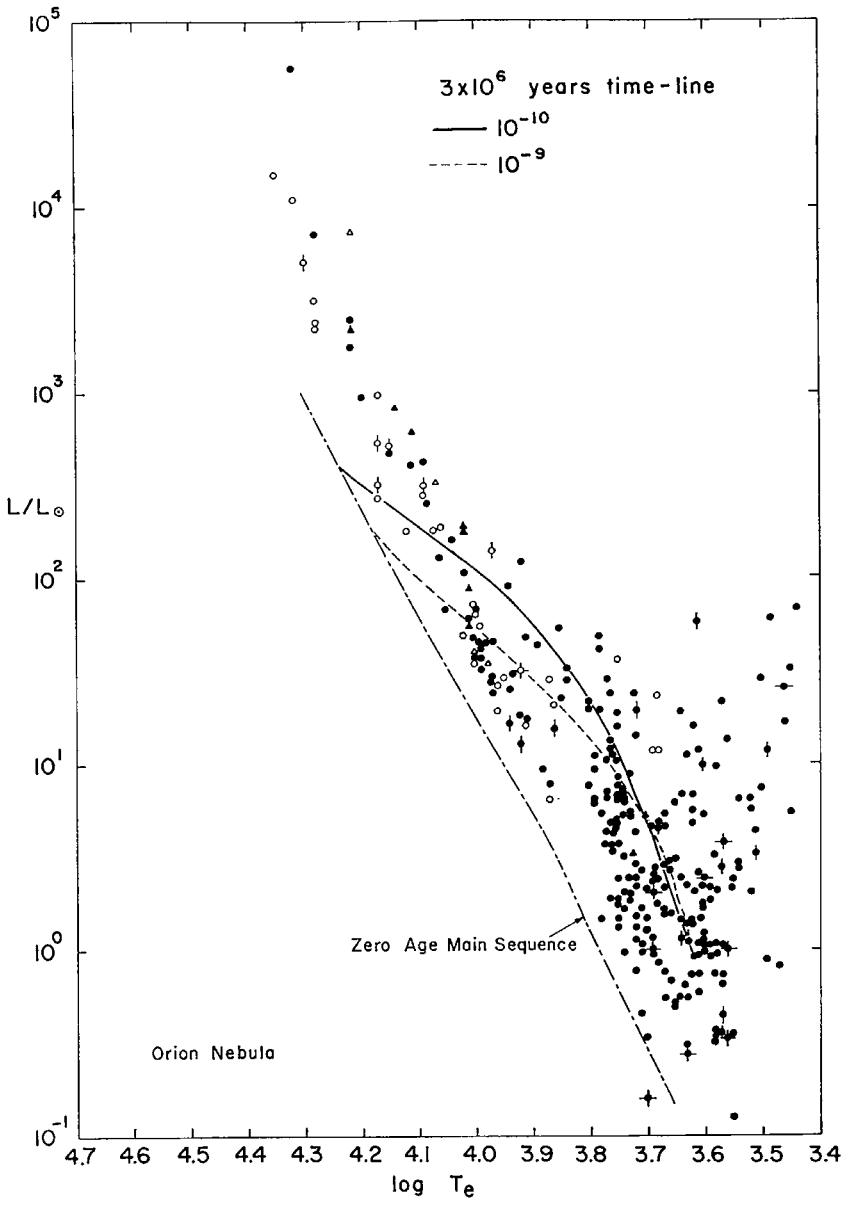

Fig. 6. The theoretical 3×10^6 yr time lines derived from the evolutionary study of the stars with different rates of mass loss, superimposed on the observed Hertzsprung-Russell diagram for the stars in the vicinity of the Orion Nebula. For further explanation, see the text.

If the more luminous of these stars are similar to those whose evolutionary tracks are plotted in Figures 2 and 3, their evolutionary age is about 10^4 yr. If they correspond to even lower mass stars, their evolutionary age is even smaller.

10. Conclusions

With mass loss relationships chosen to reproduce observational data, we have found that equal age time lines for different mass loss rates lie remarkably close to one

another in the HR diagram. From this it is concluded that the large spread of the stellar points on HR diagrams of young clusters cannot be explained as a result of variations in mass loss rate.

The most likely explanation for the spread of the points in these diagrams is a spread in the times of formation of the stars. The spread typically seems to be a few million years. This is in accord with the theoretical possibility discussed in the Introduction. Iben and Talbot (1966) suggest that NGC 2264 has an age spread of order 65 million years, but a large part of this could be due to observational and reddening dispersion.

Nevertheless, it is evident that the process of mass loss can have major effects on pre-main sequence evolution. The semi-empirical relationship used here may also be useful for post-main sequence studies, where mass loss effects are also likely to be very important.

Since the above work was completed, another study of pre-main sequence evolution with mass loss has been published (Kuhi and Forbes, 1970). A much simpler assumption was made concerning the mass loss, but nevertheless similar conclusions were reached.

Ackowledgements

We wish to thank Mr. M. Cane and Mr. M. Pine for their great assistance in rewriting the Stellar Evolution program and carrying out the calculations with mass loss. Our thanks also to Silvia Steward for her assistance, especially in running the Institute Opacity Code.

This research has been supported in part by the National Science Foundation and the National Aeronautics and Space Administration.

Note added in proof: K. M. Strom, S. E. Strom, and J. Yost (preprint) have determined that much of the spread in the positions of the stars in the pre-main sequence domain of the HR diagram of NGC 2264 is due to variations in dust absorption, and they have speculated that these stars may in fact be contained in a narrow strip in the HR diagram. If this is correct, then the basis for our conclusion that the stars were formed with a spread in times of formation is removed. The calculations in this paper may then allow an estimate to be made eventually of the extent of spreads in formation times in young clusters when the real positions of the stars in their HR diagrams can be determined.

References

Bahcall, J. N. and May, R. M.: 1968, *Astrophys. J.* **152**, L17.
Bahcall, J. N. and Moeller, C. P.: 1969, *Astrophys. J.* **155**, 511.
Biswas, S., Fichtel, C. E., Guss, D. E., and Waddington, G. J.: 1963, *J. Geophys. Res.* **68**, 3109.
Cameron, A. G. W.: 1962, *Icarus* **1**, 13.
Cameron, A. G. W.: 1968, in *Origin and Distribution of the Elements* (ed. by L. H. Ahren), Pergamon Press, London.
Cameron, A. G. W.: 1969, in *Low Luminosity Stars* (ed. by S. S. Kumar), Gordon and Breach, New York.

Deutsch, A. J.: 1956, *Astrophys. J.* **123**, 210.
Deutsch, A. J.: 1960, 'Aerodynamic Phenomena in Stellar Atmospheres' *IAU Symp.* **12**, 238.
Deutsch, A. J.: 1960a, *Mem. Soc. Roy. Sci. Liège* **3**, No. 1, p. 54.
Deutsch, A. J.: 1960b, in *Stellar Atmospheres* (ed. by L. J. Greenstein), University of Chicago Press, Chicago, p. 543.
Deutsch, A. J.: 1969, in *Mass Loss from Stars* (ed. by M. Hack), D. Reidel Publ. Comp., Dordrecht, Holland.
Ezer, D. and Cameron, A. G. W.: 1965, *Can. J. Phys.* **43**, 1497.
Ezer, D. and Cameron, A. G. W.: 1967, *Can. J. Phys.* **45**, 3429.
Field, G. B.: 1969, *Comm. Astrophys. Space Phys.* **1**, 215.
Fowler, W. A., Caughlan, G. R., and Zimmerman, B. A.: 1967, *Ann. Rev. Astron. Astrophys.* **5**, 525.
Herbig, G. H.: 1962a, in *Advances in Astronomy and Astrophysics*, Vol. 1 (ed. by Z. Kopal), Academic Press, New York, p. 47.
Herbig, G. H.: 1962b, *Astrophys. J.* **135**, 736.
Herbig, G. H.: 1967, *Scientific Am.* **217**, No. 2, 30.
Iben, I., Jr. and Talbot, R. J.: 1966, *Astrophys. J.* **144**, 968.
Iben, I. Jr.: 1969, *Ann. Phys.* **54**, 164.
Johnson, H. L.: 1957, *Astrophys. J.* **126**, 134.
Johnson, H. L.: 1966, *Ann. Rev. Astron. Astrophys.* **4**, 193.
Kahn, F. D.: 1969, *Nature* **222**, 1130.
Kuhi, L. V.: 1964, *Astrophys. J.* **140**, 1409.
Kuhi, L. V.: 1966a, *J. Roy. Astron. Soc. Can.* **60**, 1.
Kuhi, L. V.: 1966b, *Astrophys. J.* **143**, 991.
Kuhi, L. V. and Forbes, J. E.: 1970, *Astrophys. J.* **159**, 871.
Lambert, D. L.: 1967, *Nature* **215**, 43.
Lambert, D. L.: 1968, *Monthly Notices Roy. Astron. Soc.* **138**, 413.
Lovell, B.: 1969, *Nature* **222**, 1126.
Morgan, W. W. and Lodén, K.: 1966, in *Vistas in Astronomy*, Vol. 8 (ed. by Arthur Beer and K. A. Strand), Pergamon Press, London, p. 83.
Parenago, P. P.: 1954, *Trudy Sternberg Astr. Inst.* **25**.
Parker, E. N.: 1963a, 'Interplanetary Dynamical Processes', Wiley, Interscience, New York, London.
Parker, E. N.: 1963b, Colloquium, Institute for Space Studies.
Parker, P. D.: 1968, *Astrophys. J.* **153**, L85.
Penston, M. V.: 1964, *Observ.* **84**, 141.
Sharpless, S.: 1952, *Astrophys. J.* **116**, 251.
Sharpless, S.: 1954, *Astrophys. J.* **119**, 200.
Sharpless, S.: 1962, *Astrophys. J.* **136**, 767.
Spitzer, L.: 1954, *Astrophys. J.* **120**, 1.
Walker, M. F.: 1965, *Astrophys. J. Suppl.* **23**, 365.
Walker, M. F.: 1957, *Astrophys. J.* **125**, 636.
Walker, M. F.: 1969, *Astrophys. J.* **155**, 447.
Watson, W.: 1969, *Astrophys. J.* **157**, 375.
Weymann, R.: 1962, *Astrophys. J.* **136**, 884.
Weymann, R.: 1963, *Ann. Rev. Astron. Astrophys.* **1**, 97.
Wilson, O. C.: 1959, *Astrophys. J.* **130**, 499.
Wilson, O. C.: 1963, *Astrophys. J.* **138**, 832.